*Desalination and Water Treatment*
www.deswater.com
doi: 10.1080/19443994.2013.800672

51 (2013) 3979–3987
May

Taylor & Francis
Taylor & Francis Group

# Preparation and properties of polysulfone/polyacrylonitrile blend membrane and its modification with hydrolysis

Xuliang Zhang, Changfa Xiao*, Xiaoyu Hu

*State Key Laboratory of Hollow Fiber Membrane Materials and Processes, Tianjin Polytechnic University, Tianjin 300387, China*
*Email: xiaotjpu@163.com*

Received 3 May 2012; Accepted 3 April 2013

ABSTRACT

In this work, the polysulfone (PSf)/polyacrylonitrile (PAN) blend membranes were prepared via the phase inversion method induced by immersion precipitation. The PSf/PAN blends show the partial compatibility because of the different solubility parameter of polymers and DMA test results, making the interface microvoid structure for the blend membranes easy to induce. The water permeability of the PSf/PAN blend membranes is better than that of the pure PSf membrane. The contact angle measurements indicate that the hydrophilicity of PSf/PAN membranes increases with an increase in PAN concentration in the casting solution. Furthermore, the PSf/PAN blend membranes were modified with hydrolysis in sodium hydroxide solution. Characterizations of the hydrolyzed membranes, such as pure water flux and mean pore size, are better than before. Flux recovery ratios in the protein solution increase from 49.2 to 79.5% after hydrolysis.

*Keywords:* PSf/PAN; Blend; Interface microvoids; Hydrolysis; Flux recovery ratio

## 1. Introduction

Polysulfone (PSf) membranes have high mechanical property and good chemical stability. However, PSf membranes have severe fouling and low permeate flux during UF, which partially results from the hydrophobic property of PSf material [1]. Although pure water fluxes with ultrafiltration and microfiltration can be very high, flux with actual feed streams, such as protein solutions, are often significantly lower. The mechanisms, such as adsorption and pore blocking or plugging, are contributed to cause the flux to decline [2]. The main factor enhancing the adsorption of the protein into the membrane surface is hydrophobic interaction between the surface of the membranes and protein molecules [3]. Many researchers have followed the idea of increasing the hydrophilicity of a membrane material with the goal of reducing fouling. A number of methods, such as plasma treatment [4] and graft [5], can improve the hydrophilic of membranes and so on.

Blending is an important method to obtain new properties of polymeric materials with less complicate and expensive. With good stability and relatively hydrophilic, polyacrylonitrile (PAN) is widely used in the industry for membrane preparation. A majority of studies have extensively investigated the PAN-based

*Corresponding author.

*Presented at the 2012 Qingdao International Desalination Conference June 26–29, 2012, Qingdao, China*

blend membranes. Ling et al. [6] prepared the PAN/PS blend membranes and found out that their flux is higher than that of the PAN membrane. Amirilargani et al. [7] studied the hydrophilicities of PES/PAN blend membranes and found out that the performance of the membrane improves in a certain composition of PES/PAN/PEG. Furthermore, PAN is relatively active to be much easier modified by alkaline hydrolysis. Reddy and Patel [8] improved the PES/PAN blend membranes fouling resistance by treatment with aqueous alkali solutions. The unmodified and modified membranes were characterized using aqueous solutions of inorganic solutes (NaCl) and organic solutes (Polyethylene glycol [PEG]). In the past, a few studies have dealt with PSf/PAN or PES/PAN blends; they only paid more attention to enhance the surface hydrophilicity of the PSf membrane to improve their antifouling property. However, pore blocking may be dominant in the neat PES membrane, and protein adsorption on the small pores of PES/PAN blend membranes can result in pore plugging and contraction during UF [7]. In this study, the formation of interface microvoids of PSf/PAN membranes and the antifouling properties of membranes changed after modification of hydrolysis are needed to be further studied. PSf/PAN blend membranes were prepared using phase inversion method. Blending with the PAN can improve both the hydrophilicity of the PSf membrane and the quantities of interface microvoids generated during the process of phase separation, which is due to the partial compatibility of PSf/PAN blend. The effect of hydrolysis on membranes was possible to inhibit irreversible adsorption of protein and pore blocking, which improved the permeability and antifouling ability of PSf/PAN blend membranes. The morphology and performance of these membranes were investigated using field emission scanning electron microscope (FESEM), Fourier transform infrared spectroscopy (FTIR), contact angle goniometer, and element analysis.

## 2. Experimental

### 2.1. Materials

PSf was obtained from Dalian Polysulfone Plastic Limited Company. PAN (Mw = 50,000) was purchased from Shandong Qilu Petrochemical acrylic factory. N, N-dimethylacetamide (DMAc > 99%) was obtained from the Institute of Membrane Science and Technique, Tianjin Polytechnic University. PEG (reagent grade, Mw = 600) supplied by Tianjin Chemical Reagent Plant.

Table 1
Composition of casting solution

| Prepared membrane | PSf (wt.%) | PAN (wt.%) | PEG (wt.%) | DMAc (wt.%) |
|---|---|---|---|---|
| M0 | 20 | 0 | 8 | 72 |
| M1 | 18 | 2 | 8 | 72 |
| M2 | 16 | 4 | 8 | 72 |
| M3 | 14 | 6 | 8 | 72 |

### 2.2. Preparation of PSf/PAN membranes

Membranes were prepared via phase inversion method. The casting solutions consisting of PSf and PAN were prepared by blending the two polymers at different compositions (Table 1) in the presence of additive, pore former, PEG600 in a polar solvent, and DMAc, under constant mechanical stirring in a three-necked round-bottom flask for 4 h at 85˚C. The solutions were cast using a film applicator on a glass plate substrate. Then, the casted films were moved to distilled water coagulation bath for immersion precipitation and kept for 24 h before the test. All of the membranes were prepared under environmental humidity of 60% and a temperature of 25˚C. Then, some of these membranes were hydrolyzed by immersing into the aqueous solutions of sodium hydroxide. After hydrolyzing for 1 h with 8% of sodium hydroxide solutions at 75˚C, the membranes were taken out and rinsed with distilled water until the pH values reached neutral. The PSf/PAN (100/0, 90/10, 80/20, and 70/30) membranes were labeled as M0, M1, M2, and M3, respectively. The hydrolyzed PSf/PAN (100/0, 90/10, 80/20, and 70/30) membranes were designed as M0-H, M1-H, M2-H, and M3-H, respectively.

### 2.3. Membrane characterization

#### 2.3.1. Morphology examination

The morphology of the membranes was observed using FESEM (X4800, Hitachi, Japan). The samples were frozen in liquid $N_2$, followed by fracturing to expose their cross-sectional areas. Thereafter, they were sputtered with gold and recorded using FESEM.

#### 2.3.2. DMA characterization

The mechanical properties were determined using DMA (DMA242C, Netzsch, Germany) from room temperature to 250˚C at a heating rate of 5˚C $min^{-1}$, and the frequency was 1 Hz.

#### 2.3.3. Membrane permeability

The pure water flux of the membranes was determined by the following Eq. (1). The pressure difference across the membrane is 0.1 MPa.

$$J = \frac{V}{S \times t} \tag{1}$$

where $J$ is the pure water flux ($L\,m^{-2}\,h^{-1}$), $V$ is the quantity of the permeate (L), $S$ is the membrane area ($m^2$), and $t$ is the testing time (h).

Pure water flux decline ratio (FDR) values were computed from the following Eq. (2):

$$\text{FDR}\ (\%) = \frac{J_{w1} - J_{wi}}{J_{w1}} \times 100\% \tag{2}$$

where $J_{w1}$ is the pure water flux in 10 min and $J_{wi}$ is the pure water flux in $i$ minutes.

*2.3.3.1. Protein solution ultrafiltration.* Membrane fouling behaviors were studied as follows. First, pure water flux of the membrane ($J_{w1}$) was tested under the condition of 0.1 MPa TMP. Then, $3.0\,g\,L^{-1}$ egg albumen solution was fed into the filtration system. After the 30 min protein solution ultrafiltration, the membrane was flushed with pure water for 10 min, and the water flux of the membrane after being flushed was measured ($J_{w2}$). Flux recovery ratio (FRR) value was calculated using Eq. (3) to evaluate the antifouling property of the membrane.

$$\text{FRR}\ (\%) = \frac{J_{w2}}{J_{w1}} \times 100\% \tag{3}$$

#### 2.3.4. FTIR characterization

FTIR spectra were obtained using a spectroscope (Bruker, Tensor37, Germany) spectrometer with $4\,cm^{-1}$ resolution.

#### 2.3.5. Hydrophilicity measurement

The hydrophilicity of the membrane was studied based on the contact angle, equilibrium water content of the membrane. Contact angle measurement is widely used to characterize the hydrophilic property of polymeric surfaces. The contact angle of membranes was measured using a contact angle goniometer (JY-820, Chengde Testing Machine Co., Ltd., China). The contact time was 10s and each value was averaged from eight measurements.

#### 2.3.6. Mean pore size analysis

The mean pore size was the important parameter to the membrane. The membranes can be characterized by the mean pore size obtained from filtration rate experiments using Eq. (4) [9]. This experimental principle was based on Hagen-Poisseuille equation.

$$J = \frac{\varepsilon r^2 \Delta P}{8\mu\ L} \qquad r = \sqrt{\frac{8\mu L J}{\varepsilon \Delta P}} \tag{4}$$

where $\mu$ is the viscosity of water, $L$ is the thickness of the membrane, and $\Delta P$ is the difference of the pressure across the membrane.

#### 2.3.7. The degree of hydrolysis measurement

To estimate the hydrolysis degree of the membranes, the relative content of nitrogen in membranes was examined using an element analyzer (Vario EL Cube, German). The degree of hydrolysis (DH) can be defined as the changes of the nitrogen content obtained using Eq. (5); when $N_0$ was the nitrogen content of the starting membrane and $N_t$ was the nitrogen content of the membrane after hydrolysis for $t$ hour, there are

$$\text{DH} = \frac{N_0 - N_t}{N_0} \times 100\% \tag{5}$$

## 3. Results and discussion

### 3.1. Compatibility

According to the solution theory, the compatibility of two polymers is mainly governed by the solubility parameter in a system without polar interaction and hydrogen bonding. From the theory of thermodynamics, the molar free enthalpy is given by Eq. (6)

$$\Delta G_m = \Delta H_m - T\Delta S_m \tag{6}$$

where $\Delta H_m$ is the molar enthalpy of mixing and $\Delta S_m$ is the molar entropy of mixing. The lower the value of $\Delta G_m$ is, the better compatibility the two polymers will have. For polymeric system, $\Delta S_m$ is small enough to be omitted. Thus, the compatibility of the two polymers is mainly determined using $\Delta H_m$ So, when the mixing enthalpy ($\Delta H_m$) reached the minimum, the system is compatibility. Hildebrand found that the thermodynamic compatibility among polymers can be represented by the solubility parameter ($\delta$), and $\Delta H_m$ was calculated using the following Eq. (7)

$$\Delta H_m = RT\varphi_1\varphi_2(\delta_1 - \delta_2)^2 \quad (7)$$

$\delta_1$ and $\delta_2$ are the solubility parameters of polymers. The greater the difference between $\delta_1$ and $\delta_2$, the poorer is the compatibility of the two polymers [10]. Because the $\delta$ of PSf is 12.6 and $\delta$ of PAN is 15.4 [6], the difference between $\delta$ (PSf) and $\delta$ (PAN) indicates that PSf and PAN are partially compatible.

In addition, DMA was evaluated to observe the relation between Tan$\delta$ and temperature. It is well known that the glass transition temperature ($T_g$) of a polymer is an important criterion for the compatibility of components. The sulfone with two adjacent benzene rings of the PSf is composed of highly conjugate diphenyl structure, resulting in the considerable rigidity of the molecular chains of PSf, and then, $T_g$ is almost at 230°C [11]. The flexibility of the molecular chains of PAN is better than that of PSf, although there is a strong interaction between the cyano groups. Thus, the $T_g$ of PAN is almost at 92–104°C [12]. As shown in Fig. 1(b), the storage modulus of the M1 increases rapidly at the beginning of the temperature levels, as compared with the M3 membrane. That is due to the more content of PSf in the blend membranes, the more stable molecular structure, and the more difficulties for the chain movement. With an increase in the PAN content in the blend system, the $T_g$ of PSf and PAN all move to the high temperature. First, there is a strong interaction between the cyano groups and the higher PAN content would make the molecular chains move with more difficulty. Second, the effect of entanglement between the chains of PSf and PAN increases the $T_g$. As shown in Fig. 1(a), there are two differences of $T_g$ obtained from M1 and M3, respectively. The greater difference in $T_g$ can result in the worse compatibility between the mixing system, which increases the permeability of the blend membranes because of its easy formation of the interfacial microvoid.

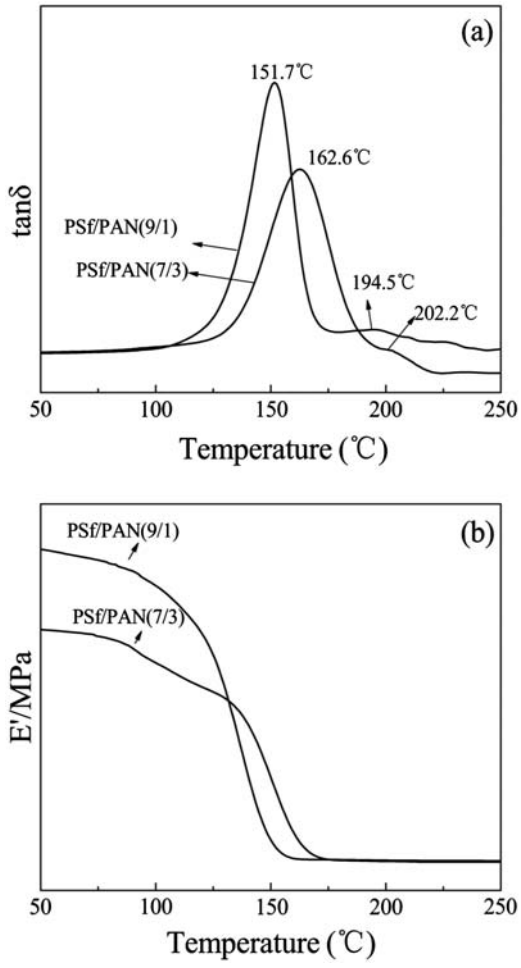


Fig. 1. DMA thermograms of PSf/PAN blend membranes.

### 3.2. Morphologies of the membranes

The FESEM images in Fig. 2 show the top surface morphology and cross-section structures of the membranes. It can be seen that the top surface of the M0 membrane is smooth and has no obvious pore structure. The pore size of the M2 membrane is denser than the M0 membranes, which have rougher top surface because the PSf/PAN blend is a partial compatibility system that can easily produce porous structure in the phase separation process. In the process of membrane solidification, the PAN is the dispersed phase that has better hydrophilic properties than PSf and the first to be separated in the coagulation bath, which is in line with the principle of forming interface microvoids structure [13]. With the increase in the PAN content, its microphase separation becomes more apparent, a greater porosity, which is favorable for the blend membrane permeability that is consistent with the water flux changes. The interface microvoid structure significantly improves the permeability of the PSf membrane.

As can be seen from the cross section in Fig. 2(a2) and (b2), the membranes have an asymmetric structure consisting of a dense top layer and a porous sublayer. M0 membrane has obviously long finger-like pore structures; however, the permeability of the membrane is poor because of the very dense sponge-like structure in its sublayer. There are much more interfacial microvoids in the cross section of the blend membranes, which are formed by the partial compatibility between PSf and PAN in the phase separation. With the gradual increase of the PAN content, there are obvious changes in the pore size, the shape of finger-like pore structure, and sublayer morphology.

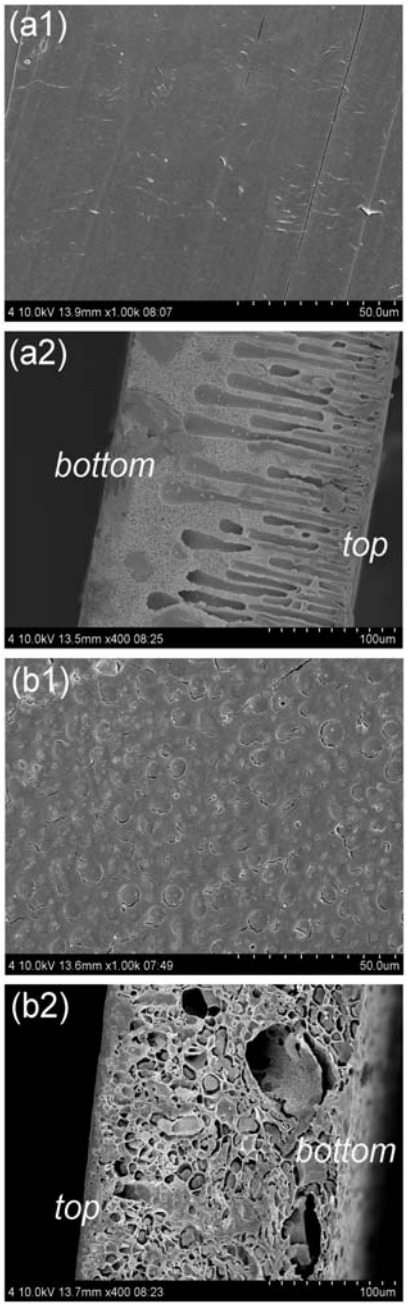


Fig. 2. FESEM graphs of the membranes with the different blend compositions: (a) M0; (b) M2; (1) top surface; (2) cross section.

Similar observations were also found by Amirilargani et al. [7]. Interactions between components in the casting solution and phase inversion kinetics have more prominent influence on the morphology of the prepared membranes. In Fig. 2(b2), there are a large number of interface microvoids in the M2 membranes and the structures are relatively loose.

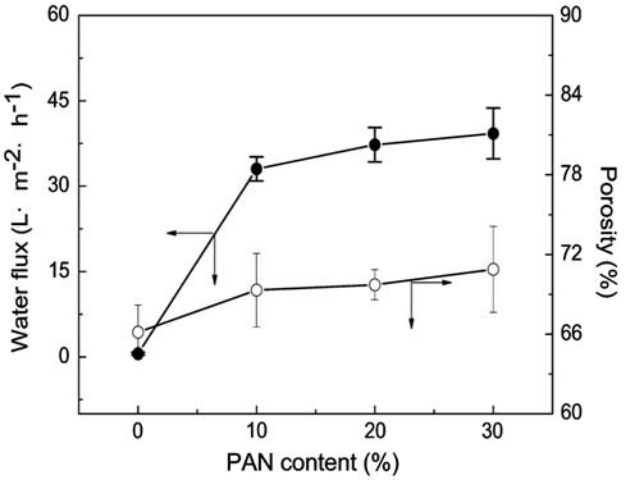


Fig. 3. The pure water flux and porosity of membranes with the different blend compositions.

### 3.3. Permeation performance of the PSf/PAN membranes

Fig. 3 shows the pure water flux and porosity increases with the increasing PAN content. As observed, the pure water flux of the blend membranes (M1, M2, and M3) has a sharp change compared with the PSf membrane. Moreover, the interface microvoid structure results in a phase separation existing in the PSf/PAN blends, effectively promoting the membrane permeability.

### 3.4. Water contact angle of the membranes

Fig. 4 shows the water contact angle of the membranes with different blend ratios. Hydrophilicity is one of the most important properties of the mem-

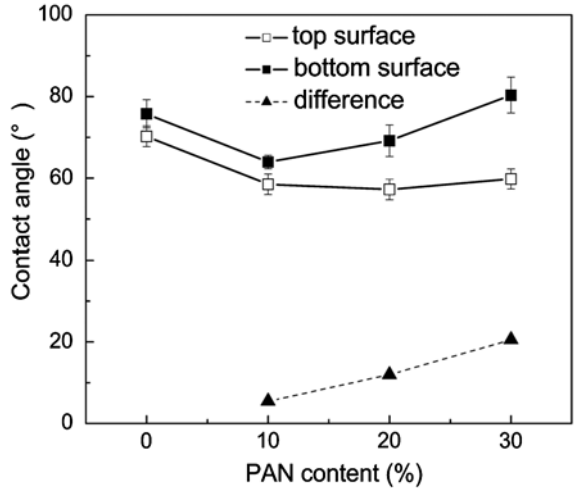


Fig. 4. The contact angle of membranes with the different blend compositions.

branes. The water contact angle data for the top surface (the coagulation bath surface) of the membranes are gradually decreasing as the PAN content increases. The pure PSf membrane has the highest water contact angle of the top surface. It indicates that the hydrophilic property of the PSf membrane is improved by blending with PAN, which has a better hydrophilicity than PSf. The water contact angle of the bottom surface (glass surface) is greater than that of the top surface, and the data have presented the wave-shaped trend. The PSf/PAN blend is a partially compatible system; it causes the phenomenon of phase separation in the coagulation bath. In contrast to PSf in the casting solution, the more hydrophilic of PAN move to the top surface, resulting in the top surface with better wet ability. The broken line in Fig. 4, shows the difference of the water contact angle between the top surface and the bottom surface. Increasing the difference of the water contact angle reduces the compatibility of the prepared blend membranes, which is beneficial to the formation of interface microvoid structure and then improves the permeability of the blend membranes.

### 3.5. Structure of the hydrolyzed membranes

Fig. 5 shows the FTIR spectra of the M2 membranes before and after hydrolysis. In the curve of a, it can be seen that the two bands at 2,243 and 1,488 $cm^{-1}$ are the characteristic absorption bands of the nitrile groups (–CN groups) [14] and the benzene groups, respectively, and the bands at 1,323 and 1,150 $cm^{-1}$ are due to the stretching vibration of $SO_2$ [15]. This indicates that there is no significant change on the characteristic absorption bands of PSf and PAN, namely, that the blend is just physics without chemical bonds. Thus, the interaction between PSf and PAN is weak. Then, the interface microvoids may be produced because of the phase separation in PSf/PAN blends.

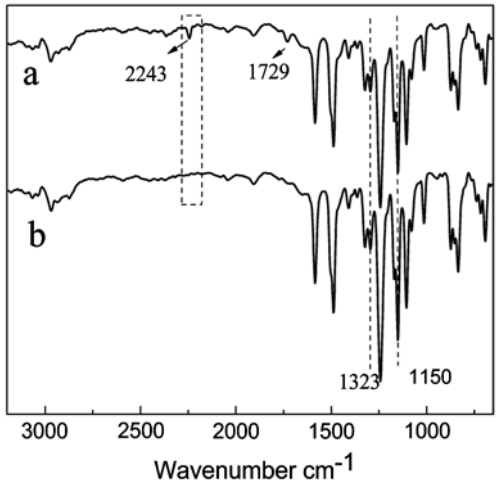


Fig. 5. FTIR spectra of the membranes: (a) M2; (b) M2-H.

After hydrolysis, the characteristic absorption bands of PSf do not have any changes as shown in Fig. 5(b). It indicates that the PSf possesses good chemical stability under the conditions of alkaline solution. During the hydrolytic process, most of the –CN groups were hydrolyzed into carboxylate groups (–COO– groups) or into amide groups (–$CONH_2$ groups) [16]. The FTIR spectrum of M2-H membrane shows that there are no nitrile groups (the band at 2,243 $cm^{-1}$ disappeared), when compared with the initial M2 membrane. The characteristic absorption band of sodium polyacrylate is at 1,584 $cm^{-1}$ that maybe overlap with the C–H original peak of PSf, so it cannot be clearly observed in Fig. 5(b). From the inherence (surface property, structure, etc.) of the composite membrane, hydrolysis takes an impact on the surface through hydrophilicity and the pore size as shown in Fig. 2 [17].

Fig. 6 shows the FESEM results of the top surface and cross-section structures of the hydrolyzed membranes. As can be seen at the top surface of the M0-H membrane without any apparent changes after hydrolysis, as a control study of FTIR, the PSf has stable performance in the alkaline solution. The top surface of the M2-H membrane images exhibit a relatively higher porosity and bigger pore size after hydrolysis. The M0-H membrane (Fig. 6(a2)) has no significant change in the cross section as compared with the M0 membrane (Fig. 2(a2)). When the hydrolysis reaction occurred, the cross section of the M2-H membrane becomes looser and appears more microporous after the interfacial microvoid disappeared. According to the mechanism of hydrolysis reaction and element analysis of the relative contents of carbon and nitrogen in the M2-H membrane, the DH of the M2-H membrane was calculated using Eq. (5) as shown in Table 2. The high DH of the M2-H membrane shows that the PAN has been hydrolyzed mostly in the alkaline solution as a dispersed phase of the PSf/PAN blend system. These changes induce a large number of cellular cavities, resulting in a larger pore size, and then improve the connectivity of the microporous structure.

### 3.6. Performance of the hydrolysis membranes

In contrast to Fig. 3, the permeability of hydrolyzed membranes has greatly improved. As shown in Figs. 7 and 8, the water flux and the mean pore size of the hydrolyzed membranes obtain greater value in PSf/PAN (8/2) blend ratio, and the porosity of the hydrolyzed membrane has lower value. The larger

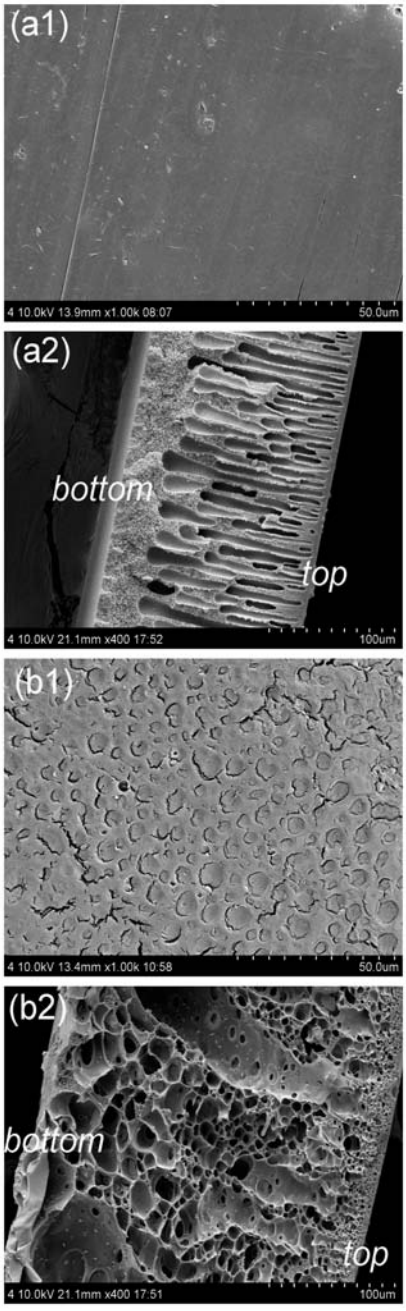


Fig. 6. FESEM graphs of the membranes with the different blend compositions: (a) M0-H; (b) M2-H; (1) top surface; (2) cross section.

pore size and better connectivity of the microporous structure in the membranes after modification (as shown in Fig. 6) increase the permeability of hydrolyzed membranes.

### 3.7. Fouling-resistant ability of membranes

The flux decline in membrane processes is due to two main sources: the concentration polarization and membrane fouling [18]. Concentration polarization can be reduced by modifying the flow over the membrane. Fouling itself can be divided into two categories: cake formation and adsorption of foulants [19]. Cake fouling is generally reversible by water flushing or back washing. Fouling because of the adsorption of foulants is essentially irreversible and highly dependent on membrane surface chemistry. As shown in

Table 2
The element analysis of M2 and M2-H membrane

| Sample | C (wt.%) | H (wt.%) | N (wt.%) |
|---|---|---|---|
| M2 membrane | 71.48 | 5.32 | 3.89 |
| M2-H membrane | 71.90 | 5.22 | 0.49 |
| | DH (%) = 87.4% | | |

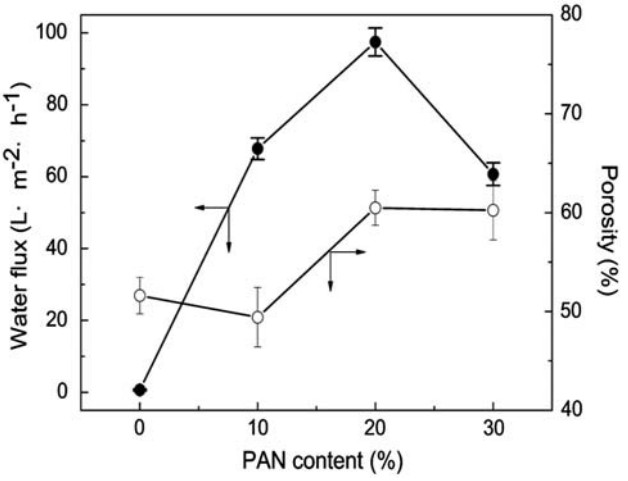


Fig. 7. The pure water flux and porosity of the hydrolyzed membranes with the different blend compositions.

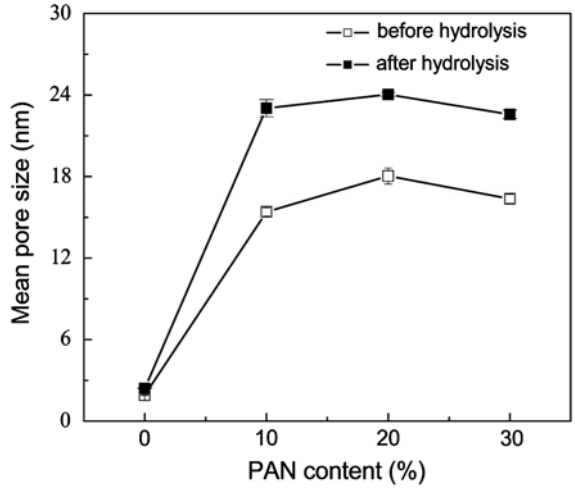


Fig. 8. The mean pore size of the membranes with the different blend compositions.

Fig. 9, the antifouling properties of membranes were characterized by the FDR values with time. After hydrolysis, first, the mean pore size of the M2-H membrane became larger; second, the M2-H membrane processes a part of sodium polyacrylate that improves the hydrophilicity of blend membranes. For porous membranes, pore size, and pore size distribution on the membrane structure are the dominating factors to flux variation, compared with the free volume in the dense polymer structure for nonporous membranes [20]. In the protein solution, the FDR values of the M2-H membranes decrease more slowly than the M2 membrane and the changes from 45.45 to 90.59% during the last time. The FRR values were taken as a measurement of the fouling resistance nature of the membrane. The higher the FRR values, the better the membrane fouling resistance. Fig. 9(b) shows that the FRR values of the M2-H membrane are higher than those of the M2 membrane without modification. On the one hand, in the cross-flow filtration when the molecules are small compared with the large pores of the membrane, the protein is not easy to gather in the membrane surface that induces membrane pore plugging [21]. Pore blocking may be dominant in the M2 membrane and decrease in the M2-H membrane because of the different pore size. The other, the adsorption of protein on the membrane surface, is physically in line with the principle of electrostatic adsorption [22]. The pH value of the feed solution is higher than the isoelectric point of the egg protein (4.5–4.9) [23], and then, the protein macromolecules would obtain more negative charges than the isoelectric point. The M2-H membrane possesses the carboxyl group, which contains negative charges similar to the protein macromolecules. Meanwhile, the adsorption of egg protein in the membranes decreases effectively because of the electrostatic action between the M2-H membrane and the protein solution.

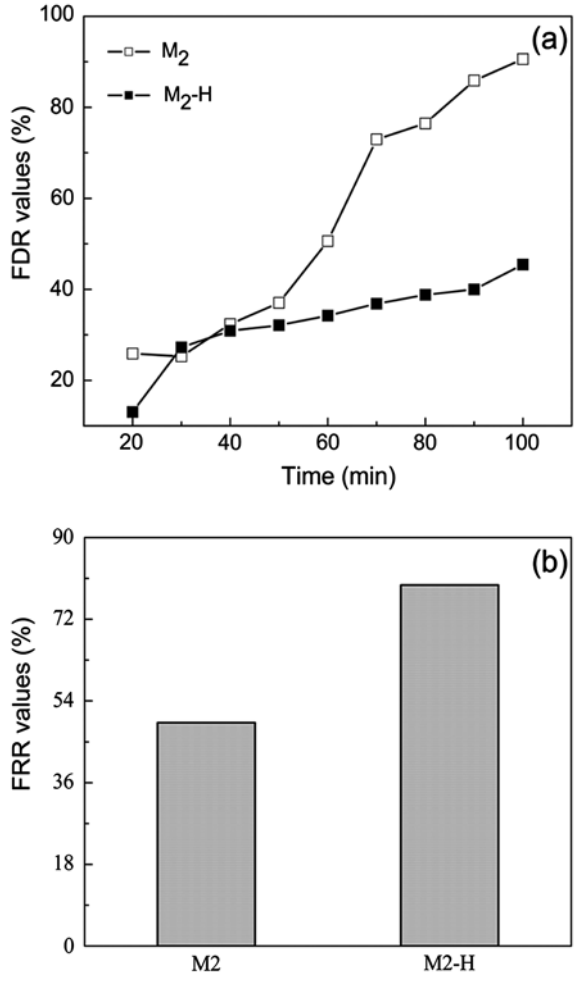


Fig. 9. The FDR and FRR values in protein solution with M2 and M2-H membranes.

## 4. Conclusion

The performance improvement of the PSf membrane by blending with the PAN was investigated. The results of this study indicate that the blend system of PSf and PAN is partially compatible; therefore, the interface microvoids are the result of the phase separation in PSf/PAN as shown in the FESEM. The water flux and the porosity increase with an increase in the PAN content. The hydrolyzed membranes have higher water flux and mean pore size. In addition, M2-H membranes can effectively reduce the FDR values in the protein solution. Moreover, the M2-H membrane shows a higher value of FRR compared with unmodified membranes.

## Acknowledgments

The authors thank the financial support of the National Basic Research Development Program of China (973 Program, 2012CB722706), the National Natural Science Foundation of China (51073120; 2127 4109), the Science and Technology Plans of Tianjin (10SYSYJC27900), and the Basic Research Program of China National Textile And Apparel Council.

## References

[1] Z. Fan, Z. Wang, N. Sun, J. Wang, S. Wang, Performance improvement of polysulfone ultrafiltration membrane by blending with polyaniline nanofibers, J. Membr. Sci. 320 (2008) 363–371.

[2] D. Möckel, E. Staude, M.D. Guiver, Static protein adsorption, ultrafiltration behavior and cleanability of hydrophilized polysulfone membranes, J. Membr. Sci. 158 (1999) 63–75.
[3] A.D. Marshall, P.A. Munro, G. Trägårdh, The effect of protein fouling in microfiltration and ultrafiltration on permeate flux, protein retention and selectivity: A literature review, Desalination 91 (1993) 65–108.
[4] M.L. Steen, L. Hymas, E.D. Havey, N.E. Capps, D.G. Castner, E.R. Fisher, Low temperature plasma treatment of asymmetric polysulfone membranes for permanent hydrophilic surface modification, J. Membr. Sci. 188 (2001) 97–114.
[5] Z. Lu, G. Liu, S. Duncan, Morphology and permeability of membranes of polysulfone-graft-poly(tert-butyl acrylate) and derivatives, J. Membr. Sci. 250 (2005) 17–28.
[6] A.l. Ling, Q. Chen, Polyacrylonitrilic/polysulfone (PAN/PS) blend ultrafiltration (UF) membranes, Desalination 101 (1995) 51–56.
[7] M. Amirilargani, A. Sabetghadam, T. Mohammadi, Polyethersulfone/polyacrylonitrile blend ultrafiltration membranes with different molecular weight of polyethylene glycol: Preparation, morphology and antifouling properties, Polym. Adv. Technol. 23 (2012) 398–407.
[8] A.V.R. Reddy, H.R. Patel, Chemically treated polyethersulfone/polyacrylonitrile blend ultrafiltration membranes for better fouling resistance, Desalination 221 (2008) 318–323.
[9] M. Zhang, Q.T. Nguyen, Z. Ping, Hydrophilic modification of poly (vinylidene fluoride) microporous membrane, J. Membr. Sci. 327 (2009) 78–86.
[10] X.Y. Hu, C.F. Xiao, S.L. An, G.X. Jia, Study on the interfacial micro-voids of poly(vinylidene difluoride)/polyurethane blend membrane, J. Mater. Sci. 42 (2007) 6234–6239.
[11] J. Zhang, J. He, Interfacial compatibilization for PSF/TLCP blends by a modified polysulfone, Polymers 43 (2002) 1437–1446.
[12] D.-G. Yu, W.-L. Chou, M.-C. Yang, Effect of draw ratio and coagulant composition on polyacrylonitrile hollow fiber membranes, Sep. Purif. Technol. 52 (2006) 380–387.
[13] C.F. Xiao, Z.F. Liu, Microvoid formation of acrylic copolymer (PAC)/cellulose acetate (CA) blend fibers, J. Appl. Polym. Sci. 41 (1990) 439–444.
[14] G. Zhang, X. Song, J. Li, S. Ji, Z. Liu, Single-side hydrolysis of hollow fiber polyacrylonitrile membrane by an interfacial hydrolysis of a solvent-impregnated membrane, J. Membr. Sci. 350 (2010) 211–216.
[15] K. Sahre, T. Hoffmann, D. Pospiech, K.-J. Eichhorn, D. Fischer, B. Voit, Monitoring of the polycondensation reaction of bisphenol A and 4,4´-dichlorodiphenylsulfone towards polysulfone (PSU) by real-time ATR–FTIR spectroscopy, Eur. Polym. J. 42 (2006) 2292–2301.
[16] L. Yu, D. Yan, G. Sun, L. Gu, Preparation and characterization of pH-sensitive hydrogel fibers based on hydrolyzed-polyacrylonitrile/soy protein, J. Appl. Polym. Sci. 108 (2008) 1100–1108.
[17] S. Mei, C. Xiao, X. Hu, W. Shu, Hydrolysis modification of PVC/PAN/SiO2 composite hollow fiber membrane, Desalination 280 (2011) 378–383.
[18] A. Asatekin, S. Kang, M. Elimelech, A.M. Mayes, Anti-fouling ultrafiltration membranes containing polyacrylonitrile-graft-poly(ethylene oxide) comb copolymer additives, J. Membr. Sci. 298 (2007) 136–146.
[19] N. Hilal, O.O. Ogunbiyi, N.J. Miles, R. Nigmatullin, Methods employed for control of fouling in MF and UF membranes: A comprehensive review, Sep. Sci. Technol. 40 (2005) 1957–2005.
[20] M. Amirilargani, T. Mohammadi, Preparation and characterization of asymmetric polyethersulfone (PES) membranes, Polym. Adv. Technol. 20 (2009) 993–998.
[21] M. Meireles, P. Aimar, V. Sanchez, Effects of protein fouling on the apparent pore size distribution of sieving membranes, J. Membr. Sci. 56 (1991) 13–28.
[22] X. Li, X. Fu, Effect of solution chemistry on membrane resistance and flux decline, Filtr. Sep. 39 (2002) 32–39.
[23] H. Per-Olof, Precipitation of egg white proteins below their isoelectric points by sodium dodecyl sulphate and temperature, Biochim. Biophys. Acta, Protein Struct. 579 (1979) 73–87.